

## EFFECT OF GRINDING ON THERMAL REACTIVITY OF CERAMIC CLAY MINERALS

V. Balek<sup>1\*</sup>, L. A. Pérez-Maqueda<sup>2</sup>, J. Poyato<sup>2</sup>, Z. Černý<sup>1</sup>, V. Ramírez-Valle<sup>2</sup>, I. M. Buntseva<sup>3</sup> and J. L. Pérez-Rodríguez<sup>2</sup>

<sup>1</sup>Institute of Inorganic Chemistry, Academy of Sciences of the Czech Republic, 250 68 Rez, Czech Republic

<sup>2</sup>Institute of Materials Sciences, CSIC-University of Sevilla, c. Americo Vespucio s/n, 41092 Sevilla, Spain

<sup>3</sup>Chemical Faculty, Moscow State University, 199234 Moscow, Russia

The effect of grinding on thermal behavior of pyrophyllite and talc as commonly used ceramic clay minerals was investigated by DTA, TG, emanation thermal analysis (ETA), B.E.T. surface area (s.a.) measurements, X-ray diffraction (XRD) and scanning electron microscopy (SEM).

A vibratory mill was used in this study, grinding time was 5 min. It was found that the grinding caused an increase in surface area and a grain size reduction of the samples. From TG and DTA results it followed that grinding caused a decrease of the temperature at which the structure bound OH groups released. The formation of high temperature phases was enhanced with the ground samples. For the ground talc sample the crystallization of non-crystalline phase into orthorhombic enstatite was observed in the range of 800°C. For ground pyrophyllite a certain agglomeration of grains was observed in the range above 950°C. Moreover, for both clays the ETA characterized a closing up of subsurface irregularities caused by grinding as a decrease of the emanation rate in the range 250–400°C. The comparison of thermal analysis results with the results of other methods made it possible to better understand the effect of grinding on the ceramic clays.

**Keywords:** DTA, emanation thermal analysis, grinding, pyrophyllite, scanning electron microscopy, surface area, talc, thermogravimetry, X-ray diffraction

### Introduction

Pyrophyllite and talc are the most common clay minerals used as raw materials in the production of ceramics. Grinding has been used to make suitable size of particles in order to control the reactivity of the raw materials. Dry grinding leads to random delamination of the silicate layers, to a strong structural alteration with important particle size reduction and to increase of surface area [1]. Several authors used SEM, TEM and other experimental techniques to demonstrate that the gradual particle size reduction and associated morphological changes took place during grinding of the clay samples [2–6]. It was observed that at the beginning of grinding the original stacking layers were delaminated and the lamellar phyllosilicate mineral particles with well-formed faces were broken by a mechanical impact, resulting in a decrease of particle size and in surface area increase. An agglomeration of particles of clay minerals by a so-called cold-welding was observed by SEM [2–7].

It was demonstrated by XRD patterns that structure disorder of the talc and pyrophyllite increased by grinding [2, 3, 5, 6]. Moreover, it was found that by increasing the grinding time amorphous material can be obtained [1]. The grinding caused significant modifications in thermal reactivity of clays. The thermal be-

haviour of ground clay minerals has been studied by several authors [1–8]. Nevertheless, different experimental methods should be used in the characterisation of mechanically treated sample in order to better understand the effect of grinding on ceramic clays.

In this study the effect of grinding on pyrophyllite and talc was investigated by DTA, TG, emanation thermal analysis (ETA), surface area measurements (BET), X-ray diffraction and scanning electron microscopy (SEM).

### Experimental

#### Samples

The natural pyrophyllite from the Hilsboro locality was supplied by Ward's N.S.Est. Inc. Rochester, NY, USA. Chemical composition of the sample is given in [2]. Talc from Puebla de Lillo (Leon, Spain) of the chemical composition given in [4] was used to produce ground samples. A vibratory mill (HERZOG, Type HSM 100) was used. Grinding time was 5 min.

#### Methods

Surface area was measured by using N<sub>2</sub> adsorption by means of the equipment Micrometrics 2200 A Model, Norcross GA (USA). The samples were out-gassed at

\* Author for correspondence: bal@ujv.cz

200°C for 12 h. The surface area (s.a.) was determined by using B.E.T. method.

Differential thermal analysis (DTA) and thermogravimetry (TG) were performed in air at a heating rate 10 K min<sup>-1</sup> up to 1100°C by using Seiko TG/DTA 6300 equipment. Emanation thermal analysis (ETA) measurements were performed on heating in air at a heating rate of 6 K min<sup>-1</sup>, using a modified NETZSCH ETA-DTA 404 instrument. Details of the ETA measurements and data treatment have been described elsewhere [9, 10]. The ETA [9–13] involves measurements of radon release rate from samples previously labelled. The specific activity of the samples after labelling was 10<sup>5</sup> Bq g<sup>-1</sup>. The <sup>224</sup>Ra and <sup>220</sup>Rn atoms were incorporated into the sample due to recoil energy (85 keV atom<sup>-1</sup>), which the atoms gained by the spontaneous  $\alpha$ -decay. The maximum depth of <sup>220</sup>Rn penetration was 80 nm as calculated with Monte Carlo method using TRIM code [13]. The rate of radon release from the sample (called also the emanation rate,  $E$ ) can be expressed in a simplified way as follows [14]:

$$E = E_{\text{recoil}} + E_{\text{diffusion}} = S[K_1 + (D/\lambda)^{1/2} K_2] \quad (1)$$

where  $E_{\text{recoil}}$  is the part of the radon release due to recoil,  $E_{\text{diffusion}}$  is the diffusion part of the released radon,  $S$  is surface area,  $K_1$  is temperature independent constant, proportional to the penetration depth of Rn recoiled atoms,  $D$  is coefficient of radon diffusion in the sample,  $\lambda$  is the decay constant of Rn,  $K_2$  is constant depending on temperature. Consequently, an increase in the radon release rate ( $E$ ) may characterize an increase of the surface area of the interfaces, whereas the decrease in  $E$  may reflect processes like closing up structure irregularities that serve as paths for radon migration, closing pores and/or a decrease in the surface area of the interfaces [14, 15].

XRD diffraction patterns were measured using the equipment Siemens Kristalloflex D-501. The diffractometer with CuK $\alpha$  radiation 40 kV and 40 mA was used. From the XRD data of the particle size of the samples was calculated by using of Scherrer equation [16]. SEM micrographs were obtained by using JEOL equipment, model JSM 5400.

## Results and discussion

### Pyrophyllite

It was determined by B.E.T. method that the surface area of the pyrophyllite sample before grinding was 1 m<sup>2</sup> g<sup>-1</sup>; the grinding caused an increase of the surface area to 52 m<sup>2</sup> g<sup>-1</sup>. From DTA and TG results (Fig. 1) it followed that the grinding caused a decrease of the temperature at which the structural OH

groups were released. The endothermal DTA effect for ground pyrophyllite was shifted to 575°C, whereas for the unground sample it was 800°C; in both cases the DTA effects were accompanied by a sample mass loss. A mass loss was observed by TG in the range up to 200°C, due to delamination of OH groups from broken edges of the ground sample. At elevated temperatures the formation of high temperature phases indicated by DTA as an exothermal effect, was enhanced for the ground sample. The XRD patterns (Fig. 2) indicated that due to grinding an increase in structure disorder took place. Moreover, by

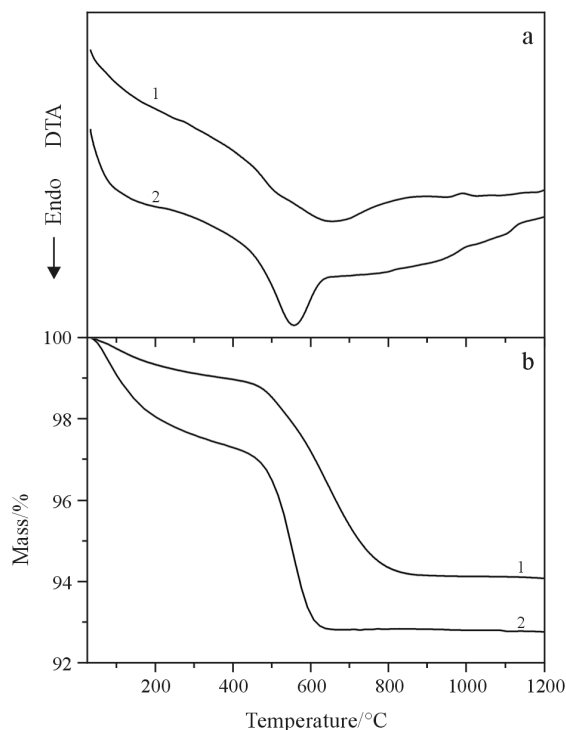


**Fig. 1** Results of a – DTA and b – TG of pyrophyllite samples measured during heating. 1 – unground sample, 2 – ground sample

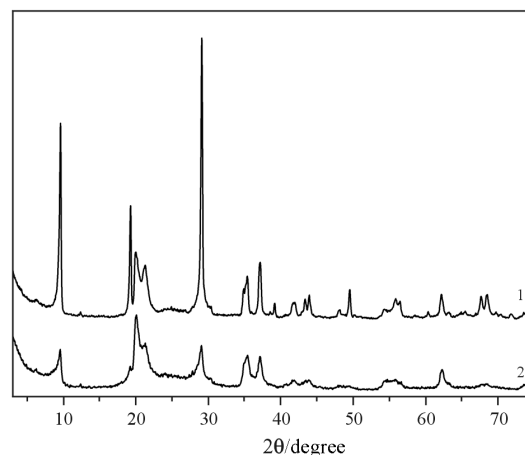


**Fig. 2** XRD patterns of pyrophyllite samples. 1 – unground sample, 2 – ground sample

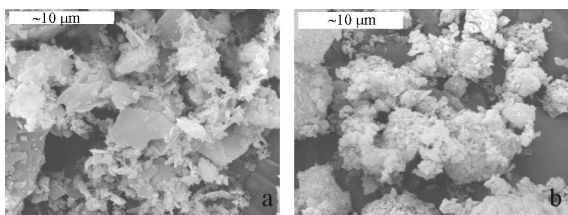


**Fig. 3** SEM micrographs of pyrophyllite samples: a – unground sample, b – ground sample

increasing the grinding time an amorphous material could be formed [1].

SEM micrographs presented in Fig. 3 confirmed the surface area results that particle size decreased due to grinding of pyrophyllite. Moreover, from Fig. 3 it followed that an agglomeration of particles in the ground sample took place.

It followed from ETA results in Fig. 4 that in both ground and unground pyrophyllite samples an increase in the emanation rate,  $E$ , took place in the range 50–250°C, due to migration of radon along micro cracks and micro pores.

The unground pyrophyllite sample was characterized by ETA in the range 25–250°C by an increasing mobility of radon atoms along natural cracks. The decrease of emanation rate,  $E(T)$ , in the range 250–380°C indicated a closing up of cracks that served as paths for radon migration. Differences in microstructure development during thermal treatment of ground and unground pyrophyllite samples were characterized by ETA as follows: The increase of  $E(T)$  in the range 500–900°C observed with the unground sample corresponds to a liberation of structural OH that is characterized by an enhanced mobility of radon along grain boundaries. The decrease of the emanation rate was observed in the range above 950°C due to a decrease of the number of grain boundaries that served as paths for radon migration. On contrary, for the ground pyrophyllite sample only

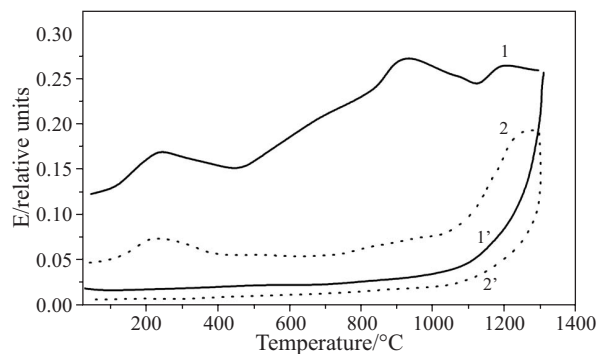


**Fig. 4** Results of ETA of unground and ground pyrophyllite samples measured during heating (curves 1 and 2) and cooling (curves 1' and 2'). Curves 1 and 1' – correspond to the unground sample, curves 2 and 2' – correspond to the ground sample

**Table 1** Radon permeability in pyrophyllite heated to 1300°C

Samples	Cooling in the range 1300–30°C	
	Radon permeability characteristics	
	$Q/kJ\ mol^{-1}$	$k_D/s^{-1}$
1 – non ground	169	13.50
2 – ground	146	0.18

a slight increase of  $E$  was observed in the range of 500–900°C due to agglomeration of the grains. However, in the range 1000–1250°C an enhanced radon release was observed by ETA in both unground and ground samples due to formation of new phases. This interpretation is in agreement with our previous statements [17].

Table 1 presents the characteristics of radon diffusion, namely the values of  $Q$  and of the constant  $k_0$  obtained by a mathematical modeling from experimental ETA results of non-ground and ground pyrophyllite samples (Fig. 4, curves 1' and 2'). Equation (2) was used for the modeling and calculations.

It followed from Table 1 that the samples obtained after heating to 1300°C possessed a slightly lower value of the activation energy of radon diffusion when the starting material was ground that when the non ground initial was used. The differences in the radon permeability are not significant, so it can be assumed that the number of radon diffusion paths in the heated samples did not considerably differ for these two samples and the effect of grinding on the properties of the pyrophyllite sample was not significant when the sample was heated to 1300°C.

#### Mathematical modeling

The temperature dependence of the radon release rate obtained by the ETA was used for the evaluation of the permeability and microstructure development characterization.

In the modeling the following expression was used for radon release rate due to diffusion

$$E_D(T) = A \left[ \frac{1}{k_{D_0} \exp\left(-\frac{Q_D}{RT_0}\right) + \lambda_{Rn}} - \frac{1}{k_{D_0} \exp\left(-\frac{Q_D}{RT}\right) + \lambda_{Rn}} \right] \quad (2)$$

where  $\lambda_{Rn} = 1.2464 \cdot 10^{-2} [s^{-1}]$  is the decay constant of  $^{220}\text{Rn}$ ,  $A = \lambda_{Ra} C_{Ra}$  is a coefficient of concentration transformation,  $\lambda_{Ra} = 2.2035 \cdot 10^{-6} [s^{-1}]$ ,  $k_D$  – rate constant of radon desorption, depending on temperature according to Arrhenius relationship,

$$k_D = k_{D_0} \exp(-Q_D/RT)$$

where  $Q_D$  is activation energy of radon desorption,  $R=8.3096$  [J mol<sup>-1</sup> K<sup>-1</sup>] is molar gas constant.

### Talc

It was found that the surface area of the natural talc sample before grinding was 3 m<sup>2</sup> g<sup>-1</sup> and that it increased after grinding to 110 m<sup>2</sup> g<sup>-1</sup>. From DTA and TG results (Fig. 5) it followed that thermal behavior of ground and unground samples of talc was similar up to 800°C, but it differed on heating above 800°C. However, the presence of sorbed water due to OH groups on the broken edges of particles of the ground sample was detected by mass decrease in the range from 30 up to 150°C.

In the DTA curve of the ground talc sample (Fig. 5a) an exothermal effect at 830°C characterized the structure changes due to crystallization of non-crystalline phases, formed by grinding of natural talc sample, into orthorhombic enstatite [18]. The mass loss in the range 800–1000°C due to dehydroxylation was observed by TG (Fig. 5b). For the unground sample the mass loss due to dehydroxylation took place in range 900–1050°C and no exothermal DTA effect was observed, in contrary to the ground sample. Consequently, the grinding enhanced the formation of high temperature phases in talc.

The XRD patterns presented in Fig. 6 confirmed that structure disorder of the ground samples in-

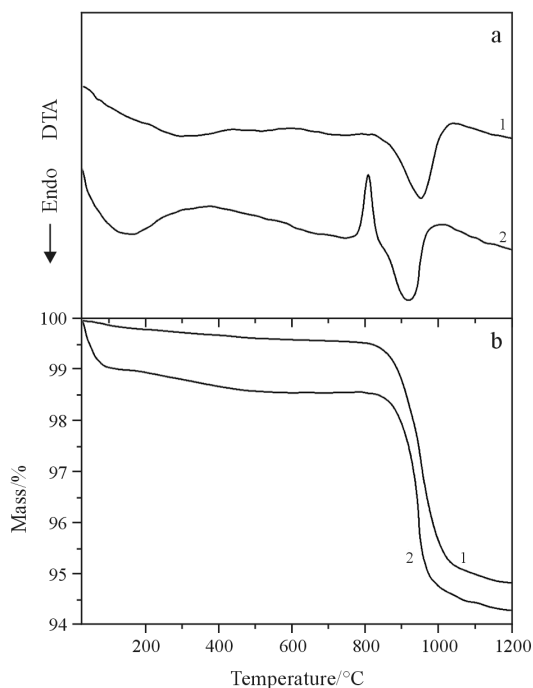


**Fig. 5** Results of a – DTA and b – TG of talc samples measured during heating. 1 – unground sample, 2 – ground sample

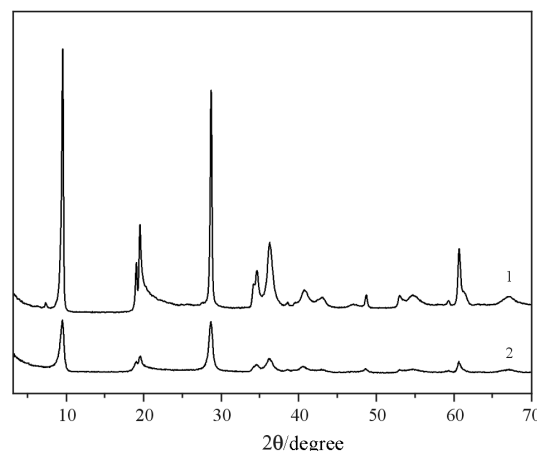


**Fig. 6** XRD patterns of talc samples. 1 – unground sample, 2 – ground sample

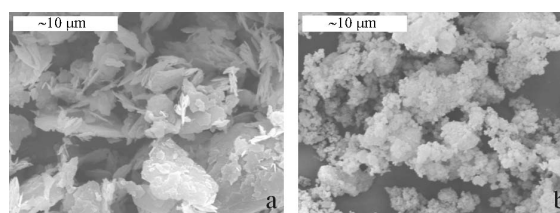


**Fig. 7** SEM micrographs of talc samples: a – unground sample, b – ground sample

creased in comparison with the unground sample. SEM micrographs in Fig. 7 confirmed the decrease of particle size with the ground sample. The ETA results of both unground and ground talc sample (Fig. 8) are in agreement with the results of surface area measurement and XRD patterns presented in Fig. 6. The increase in the emanation rate,  $E(T)$ , in the range 50–250°C is due to migration of radon along micro cracks and micro pores. The temperature of closing up the micro cracks and of the subsurface irregularities is indicated by a decrease of the emanation rate,  $E(T)$ , on heating in the range 250–450°C. The abrupt decrease of emanation rate  $E(T)$  observed with ground sample in the range of 800–870°C corresponded to the crystallization of non-crystalline phase into orthorhombic enstatite. For the unground sample no decrease of  $E$  was observed above 800°C; on the contrary, an increase of  $E(T)$  started at 800°C due to dehydroxylation of talc in bulk of the sample.

The temperature dependence of the radon release rate observed by the ETA in Fig. 8, was used for the evaluation of the permeability and microstructure development characterization.

The radon diffusion characteristics calculated from ETA results of the talc sample measured during cooling (Fig. 8, curve 1' and 2') are summarized in Table 2.

From Table 2 it follows that the unground and ground samples possessed similar values of the acti-

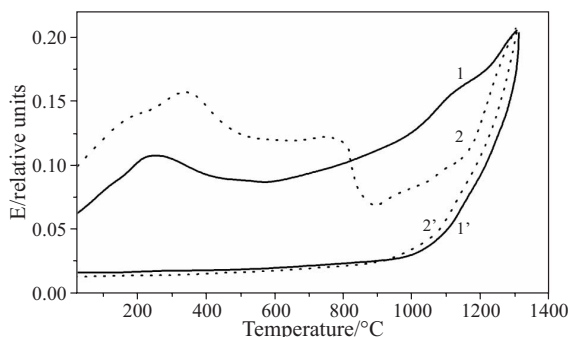


**Fig. 8** Results of ETA of unground and ground talc samples measured during heating (curves 1 and 2) and cooling (curves 1' and 2'). Curves 1 and 1' – correspond to the unground sample, curves 2 and 2' – correspond to the ground sample

**Table 2** Radon permeability in talc heated to 1300°C

Samples	Cooling in the range 1300–30°C	
	Radon permeability characteristics	
	$Q/\text{kJ mol}^{-1}$	$k_D/\text{s}^{-1}$
1 – non ground	127	10.3
2 – ground	135	3.0

vation energy  $Q$  of radon diffusion calculated from the ETA results measured during cooling of both samples. Therefore it can be assumed that the number of radon diffusion paths in the heated samples to 1300°C did not considerably differ.

## Conclusions

The effect of grinding on pyrophyllite and talc was characterized of DTA, TG, emanation thermal analysis (ETA), surface area measurements (BET), X-Ray diffraction and scanning electron microscopy (SEM). It was observed that grinding caused a decrease of the temperature at which the structure bound OH groups released and the formation of high temperature phases was enhanced with the ground samples. A mutual comparison of DTA, TG, ETA results made it possible to better understand the effect of grinding on the ceramic clays.

## Acknowledgements

This work was carried out in the frame of the bilateral cooperation between C.S.I.C and Academy of Sciences of the Czech Republic. The financial support of the Academy of Sciences of the Czech Republic (project No. AV0Z403205) and of the Ministry of Education of the Czech Republic (Projects LA-292 and ME-879) is gratefully acknowledged. The authors are grateful to the Ministry of Science and Technology

of Spain and to the FEDER program of the E.C. for financial support (grant No. MAT 2005-04838).

## References

- 1 J. L. Pérez-Rodríguez, Applied Study of Cultural Heritage (J. L. Pérez-Rodríguez, editor) C.S.I.C., Madrid 2003, p. 425.
- 2 J. L. Pérez-Rodríguez, L. Madrid Sanchez del Villar and P. J. Sánchez-Soto, Clay Miner., 23 (1988) 399.
- 3 P. J. Sánchez-Soto, M. Del Carmen Jimenez de Haro, L. A. Perez-Maqueda, I. Varona and J. L. Pérez-Rodríguez, J. Am. Ceram. Soc., 83 (2000) 1649.
- 4 P. J. Sánchez-Soto, A. Wiewiora, M. A. Aviles, A. Justo, L. A. Perez-Maqueda, J. L. Pérez-Rodríguez and P. Bylina, Appl. Clay Sci., 12 (1997) 297.
- 5 A. Wiewiora, P. J. Sánchez-Soto, M. A. Aviles, A. Justo and J. L. Pérez-Rodríguez, Appl. Clay Sci., 8 (1993) 261.
- 6 A. Wiewiora, P. J., Sánchez-Soto, M. A. Aviles, A. Justo, L. Pérez Maqueda and J. L. Pérez-Rodríguez, Int. J. Soc. Mat. Eng., 4 (1996) 48.
- 7 E. T. Stepkowska, J. L. Pérez-Rodríguez, M. C. Jiménez de Haro, P. J. Sánchez-Soto and C. Maqueda, Clay Miner., 36 (2001) 105.
- 8 V. Balek, J. L. Pérez-Rodríguez, L. A. Pérez-Maqueda, J. Šubrt and J. Poyato, J. Therm. Anal. Cal. OnlineFirst, DOI : 10.1007/s10973-005-7462-5.
- 9 V. Balek, Thermochim. Acta, 22 (1978) 1.
- 10 V. Balek and M. E. Brown, Less common techniques, Handbook on Thermal Analysis and Calorimetry, Vol. 1 Chapt. 9, Ed. by M. E. Brown, Elsevier Science B. V., 1998, p. 445.
- 11 L. A. Pérez-Maqueda, V. Balek, J. Poyato, J. L. Pérez-Rodríguez, J. Šubrt, I. M. Bountsewa, I. N. Beckman and Z. Malek, J. Therm. Anal. Cal., 71 (2003) 715.
- 12 V. Balek and J. Tölgyessy, Emanation thermal analysis and other radiometric emanation methods, in Wilson and Wilson's Comprehensive Analytical Chemistry, Part XIIC, G. Svehla Ed.; Elsevier Science Publishers, Amsterdam 1984, p. 304.
- 13 J. F. Ziegler, J. P. Biersack and U. Littmark, The Stopping and Range of Ions in Solids, Pergamon Press, New York 1985.
- 14 L. A. Pérez-Maqueda, J. M. Criado, C. Real, V. Balek and J. Šubrt, J. Eur. Ceram. Soc., 22 (2002) 2277.
- 15 N. K. Labhsetwar, V. Balek, S. Rayalu, T. Terasaka, A. Yamazaki, J. Šubrt, H. Haneda and T. Mitsuhashi, J. Therm. Anal. Cal., 80 (2005) 67.
- 16 H. P. Klug and L. E. Alexander, X-ray diffraction procedures, J. Wiley and Sons, New York, 2<sup>nd</sup> Edition, 1974, p. 687.
- 17 P. J. Sánchez-Soto, J. L. Pérez-Rodríguez, I. Sobrados and J. Sanz, Chem. Mater., 9 (1997) 677.
- 18 E. F. Aglietti and J. M. Porto Lopez, Mater. Res. Bull., 27 (1992) 1205.

DOI: 10.1007/s10973-006-8093-1